Available online at www.sciencedirect.com
ScienceDirect
Gait & Posture xxx (2007) xxx–xxx
GAIT & POSTURE
www.elsevier.com/locate/gaitpost

Uncertainties in inverse dynamics solutions: A comprehensive analysis and an application to gait

Raziel Riemer, Elizabeth T. Hsiao-Wecksler, Xudong Zhang *

Department of Mechanical and Industrial Engineering, University of Illinois at Urbana-Champaign, Urbana, IL 61801, USA

Received 17 July 2006; received in revised form 23 July 2007; accepted 29 July 2007

Abstract

This paper presents a comprehensive analysis of the uncertainties in joint torque estimates derived through inverse dynamics. The analysis considered most of the quantifiable sources of inaccuracy in the input variables for inverse dynamics solutions (i.e., errors in body segment parameter estimates, joint center of rotation locations, force plate measurements, motion capture system measurements, and segment angle calculations due to skin movement artifacts). Estimates of inaccuracies were synthesized from existing literature and from a complementary set of experimental data. The analysis was illustrated and tested via an inverse dynamic analysis of gait, in which kinematic and force plate data from 10 adult subjects were recorded and used to calculate the planar (flexion/extension) torques at the ankle, knee, hip, elbow, shoulder, and bottom of torso. The results suggested that the uncertainties in torque estimates derived through inverse dynamics can be substantial (6–232% of the estimated torque magnitude); the time-varying uncertainty patterns do not resemble the torque profiles, and the magnitudes are smaller for more distal joints; the main contributors to these uncertainties were identified to be the inaccuracies in estimated segment angles and body segment parameters. The empirical test also showed that the uncertainty predicted by a more conservative (smaller) set of inaccuracy estimates was comparable to the statistical (3σ) bound of the error. Implications in terms of how inverse dynamics solutions should be interpreted and improved, along with the limitations of the current work, are discussed.

Keywords: Error analysis; Inverse dynamics; Uncertainty

1. Introduction

Inverse dynamics is a fundamental and commonly used computational procedure for analysis of human movement. With anthropometric and kinematic information as the input, an inverse dynamics procedure calculates the force and torque reactions at various body joints [1]. Despite widespread use, it is well recognized that inverse dynamics solutions are prone to errors.

Errors can stem from a variety of sources including inaccuracies in segmental parameters (i.e., mass, moment of inertia, and center-of-mass location) [2–5], inaccuracies due to (equipment) noise in surface marker movement [6] and ground reaction force measurements [7], inaccuracies related to locating joint centers [8–10], inaccuracies in estimating center of pressure location [11,12], and inaccuracies caused by the relative motions between surface markers and underlying bones—"skin movement artifacts" [13–15]. In this work, *error* is defined as the difference between a calculated or measured value and the true value; *inaccuracy* refers to the range of the error associated with an input variable to an inverse dynamics procedure or model, whereas *uncertainty* refers to the magnitude of the maximum possible error in inverse dynamics solutions.

A comprehensive and quantitative understanding of the uncertainties in inverse dynamics solutions has not been established. Previous studies as referenced above have focused on only one or two inaccuracies. These studies typically examine the relationship between a specific inaccuracy and resulting error, i.e., perform a sensitivity analysis. Sensitivity analyses, however, do not ascertain the magnitude of error itself or the range of error, and thus do not contribute to the knowledge of uncertainty as a totality. The

* Corresponding author. Tel.: +1 412 586 3940; fax: +1 412 586 3979.
E-mail address: xuz9@pitt.edu (X. Zhang).

0966-6362/$ – see front matter © 2007 Elsevier B.V. All rights reserved.
doi:10.1016/j.gaitpost.2007.07.012

latter is what sets the confidence limit for inverse dynamics solutions, and is therefore more critical to the validity of the analysis.

A more extensive study that included multiple error sources was conducted by Desjardins et al. [16]. Their analysis included error sources caused by inaccuracies in nine input variables of an inverse dynamics model that estimated the torque at the L5/S1 joint during a lifting motion. The investigation compared an upper body model (i.e., a ''top-down'' approach) and a lower body model (i.e., a ''bottom-up'' approach requiring ground reaction force measurements). This study was limited because the magnitudes of the inaccuracies were arbitrarily set to 5% of the corresponding input variables. As a result, this approach was not a true uncertainty analysis of the joint torques.

In this study, we chose to conduct a more inclusive and systematic analysis of the uncertainties in estimated torques at major body joints. The error analysis incorporates the effects of the most commonly identified sources of error in the input variables for inverse dynamics calculations. More realistic estimates of inaccuracy magnitudes were synthesized from published data and from our own experiments when such data were not available in the literature. We demonstrate our approach via an analysis of a set of two-dimensional gait data. However, the methodology is general and could be applied to both two- and three-dimensional analyses.

2. Methods

2.1. Anthropometric linkage representation

The human body was represented by a 13-segment linkage consisting of the forearms (including the hands), upper arms, torso (including the head), thighs, shanks, feet, and two mass-less links connecting the bi-lateral shoulder and hip joints (Fig. 1). The torso segment inter-connects the midpoints of the two mass-less links. The mass-less links accounted for the effects of the distances from the hip and shoulder joint centers to the spine, necessary for calculating the torques at the bottom of the torso. The segmental properties (mass, center-of-mass and moment of inertia) were calculated based on adjustments to Zatiorsky-Seluyanov's work by De Leva [17].

This 13-segment linkage system was then divided into two models, one for the upper body and one for the lower body, separated at the bottom of the torso link. The joint torque equations for the upper body (elbow, shoulder, and torso bottom) were derived recursively starting from the hand in a ''top-down'' fashion. Equations for the lower body (ankle, knee, hip, and torso bottom) were derived recursively starting from the foot in a ''bottom-up'' fashion. The equations for the bottom-up approach incorporated ground reaction force measurements using a foot model presented by Winter [1]. The model was planar but bi-lateral (i.e., both sides represented). In the bottom-up approach, only the right-side solutions were considered (due to the limitation of one force plate we could not calculate full cycle for the left leg).

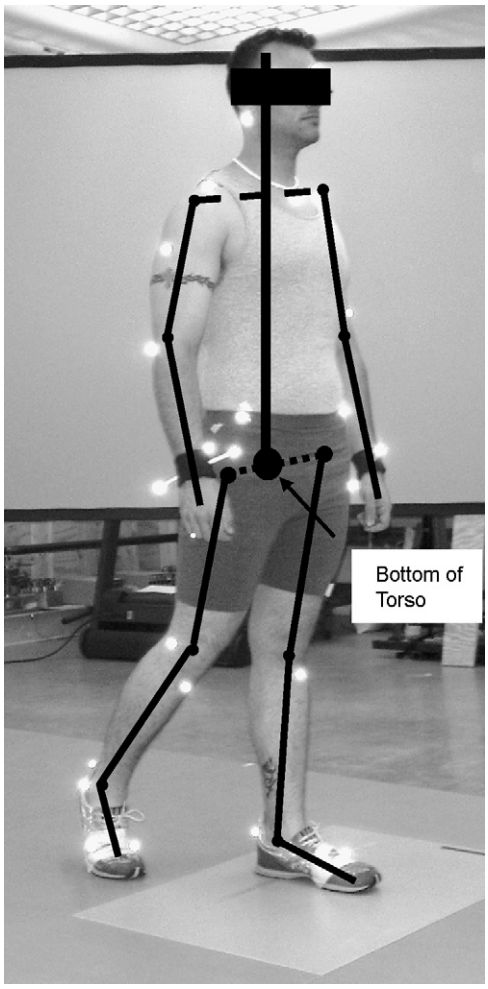

Fig. 1. The full body represented with a 13-segment linkage that allows bi-lateral motion in a 2D sagittal-plane investigation. Mass-less links (dashed lines) connect the shoulder and hip joints to the torso link. Top-down and bottom-up approaches were used to evaluate the uncertainty in torque solutions of the joint at the bottom of the torso.

2.2. Equations of motion

For both models, the equations of motion that allow for calculation of the 2D sagittal-plane (flexor/extensor) torque at joint j (τ_j) were derived recursively using the following equations:

$$m_i \boldsymbol{I}^{2\times 2} a_{ci} = \boldsymbol{f}_{j-1} - \boldsymbol{f}_j \quad (1)$$

$$I_i \theta''_i = (\boldsymbol{d}_i \times \boldsymbol{f}_{j-1}) - (\boldsymbol{p}_i \times \boldsymbol{f}_j) + \tau_{j-1} - \tau_j, \quad (2)$$

where m_i is the mass of segment i, $\boldsymbol{I}^{2\times 2}$ is a two-by-two identity matrix, $\mathbf{a}_{ci}$ is the translational acceleration vector that includes (a_x, $a_z + g$) for the center-of-mass i, $\boldsymbol{f}_j$ and $\boldsymbol{f}_{j-1}$ are force vectors at joint j and the next adjacent joint ($j - 1$) on segment i, θ''_i is the angular acceleration of segment i, I_i is the moment of inertia of the segment relative to the center-of-mass, $\boldsymbol{d}_i$ is the vector from the center-of-mass i to $\boldsymbol{f}_{j-1}$, $\boldsymbol{p}_i$ is the vector from center-of-mass i to $\boldsymbol{f}_j$, and τ_{j-1} is the torque in joint $j - 1$.

The calculated joint torques can alternatively be expressed as a function of the input variables:

$$\boldsymbol{\tau} = f(\boldsymbol{F}, \boldsymbol{L}_F, \boldsymbol{\theta}, \boldsymbol{\theta}'', \boldsymbol{a}_c, \mathbf{BSP}, t), \quad (3)$$

Please cite this article in press as: Riemer R, et al., Uncertainties in inverse dynamics solutions: A comprehensive analysis and an application to gait, Gait Posture (2007), doi:10.1016/j.gaitpost.2007.07.012

Table 1
Estimates of inaccuracy values[a] for body segment parameters including the mass, center-of-mass location, and moment of inertia

Reference	Mass (%)			Center-of-mass (%)			Moment of Inertia (%)			
	Kingma et al. [3]	Durkin et al. [25]	Ganley and Powers [5]	Kingma et al. [3]	Durkin et al. [25]	Ganley and Powers [5]	Kingma et al. [3]	Challis [2]	Durkin et al. [25][b]	Ganley and Powers [5]
Thigh	9.4	3.2	12	27.2	2.8	11	16	16.9	14.2	14
Shank	2.1	3.2	0	1.4	2.8	6	53	11.6	14.2	26
Foot	27.5	3.2	36	17.3	2.8	15	71	12.2	14.2	47
Torso	11.3	3.2		15.5	2.8		38.8		14.2	
Upper Arm	12.7	3.2		4.9	2.8		16.3	1.9	14.2	
Forearm	8.6	3.2		3.3	2.8		23.4	11.6	14.2	
Hands	13.1	3.2			2.8		1.4	11	14.2	
Head	18.5	3.2		7.3	2.8		28.4		14.2	

[a] Values based on comparison of accuracy of models (Challis [2], Durkin et al. [25]) or differences between measurement methods (Kingma et al. [3], Ganley and Powers [5]).
[b] Authors attributed most of this error to the use of the pendulum technique; by comparison, they note that use of the cylindrical geometric calculation method would result in an error of 2.63%.

where $\boldsymbol{\tau}$ is the vector of torques for all joints, $\boldsymbol{F}$ is the external force and moment vector, $\boldsymbol{L}_F$ is the vector of the locations of the applied external forces and moments, $\boldsymbol{\theta}$ is the angle vector, $\boldsymbol{\theta}''$ is the angular acceleration vector, $\boldsymbol{a}_c$ is the translational center-of-mass acceleration vector, **BSP** is the vector of body segment parameters (moment of inertia, mass, and location of center-of-mass), and t is time. Note that in this formulation we do not explicitly identify the joint center locations as input variables; rather, these locations are implicitly included in the calculation of the segmental angles and lengths.

2.3. Error analysis

An error analysis method was used to compute the effects of input variable inaccuracies on the uncertainties in the joint torques calculated via inverse dynamics. The following formulation computes the upper bound on the possible error [18]:

$$U_j = \left|\frac{\partial \tau_j}{\partial x_1}\Delta x_1\right| + \left|\frac{\partial \tau_j}{\partial x_2}\Delta x_2\right| + \cdots\cdots + \left|\frac{\partial \tau_j}{\partial x_n}\Delta x_n\right|, \quad (4)$$

where U_j is the uncertainty in the torque value at joint j (τ_j), and Δx_i is the inaccuracy associated with input variable x_i.

2.4. Determination of the inaccuracy magnitudes (Δx_i)

It is important to know the possible sources of inaccuracies and to obtain realistic estimates of their magnitudes (Δx_i). Possible sources of inaccuracies and estimates of their magnitudes were identified from the literature. The primary sources of such errors were: (1) estimates of body segment parameters; (2) segment angle calculations due to relative movement between surface markers and the underlying bone structure; (3) identification of joint center of rotation locations; (4) errors related to force plate measurements; and (5) motion marker noise and its effect on segmental accelerations (for reviews of various error sources, see [19–23]).

Although some have determined parameters such as segment mass, center-of-mass location, and moment of inertia on living subjects (e.g. [25]), these techniques require limited access equipment and thus these parameters are not readily measurable on every test subject [24]. Therefore, estimates of inaccuracies for these parameters are difficult to quantify. To overcome this problem, we used multiple sources of information to assess the magnitude of these inaccuracies. Since the reported values for Δx_i varied across previous studies, two sets of Δx_i were formed to represent the range of values: Set 1 contains the lower values of inaccuracies for each of the variables (small Δx_i), and Set 2 contains the higher values (large Δx_i).

2.4.1. Body segment parameters

Several studies provided values for inaccuracy magnitudes in body segment parameters (Table 1). Kingma et al. [3] evaluated the body segment parameter (BSP) values determined using proportional and geometric anthropometric models. Differences in the estimated segment properties were found comparable to the errors in BSP reported by Cappozzo and Berme [24] and Pearsall and Costigan [4]. Challis [2] compared nonlinear and linear proportional models for moment of inertia estimation using non-cross and cross validation. Durkin et al. [25] evaluated the accuracy of dual energy X-ray absoptiometry (DXA) as a means for measuring BSP. Hatze [26] estimated a 5% inaccuracy value for his geometric approach. Ganley and Powers [5] estimated the lower extremity anthropometric parameters using DXA, and compared them with segment properties obtained using cadaver-based estimation. Thus, for the smaller set of inaccuracies, we elected to use 5%; for the larger set of inaccuracies, values available from Ganley and Powers [5] were used, and when unavailable, the larger of the values reported by Challis [2] and Kingma et al. [3] were chosen.

2.4.2. Segment angle and skin motion artifact

The relative movements between the surface markers and the underlying bone structure, also known as skin motion artifacts, can cause errors in calculation of the segment angles (and other errors such as angular acceleration, joint center location, center-of-mass location and acceleration). Cappozzo et al. [13] examined subjects that had suffered fractures in the tibia and femur and were wearing external fixtures rigidly connected to the bone. The relative movements of surface markers and the underlying bone during walking were found to be in range of 10–30 mm. It was then concluded that the maximal errors on the flexion extension angle were in the order of 8°. Holden et al. [14] studied the error in the tibia orientation and compared the movements between a bone-mounted target set and a surface marker set. The greatest relative rotational difference about the mediolateral axis was less than 3°, and the maximum displacement error was 10.5 mm. The inaccuracies in segment angles for the upper extremities were estimated by Roux et al. [27] to be in the

Please cite this article in press as: Riemer R, et al., Uncertainties in inverse dynamics solutions: A comprehensive analysis and an application to gait, Gait Posture (2007), doi:10.1016/j.gaitpost.2007.07.012

order of 4°. Data from these studies were the bases for setting the inaccuracy values for the segmental angles (Table 3).

2.4.3. Location of joint center of rotation

Inaccuracy magnitudes related to the joint center of rotation (COR) locations were obtained from several sources. Schwartz and Rozumalski [10] proposed a new method to determine lower extremity joint centers of rotation (COR's). The estimated errors were 3–9 mm for the hip joint and 1–3 mm for the knee joint. They also compared their results with values obtained using a traditional method [28], and found that the difference between methods at the hip was up to 16.6 mm, in the knee difference was up to 7.4 mm. The differences in the estimated joint center locations were considered as the magnitudes of the inaccuracy in the joint center location. Leardini et al. [9] estimated the error magnitude for the hip joint center to be 11.8 ± 4.1 mm, while Bell et al. [8] estimated it to be 37.9 ± 19 mm (this large magnitude is attributed mostly to lack of range of motion in this study). In our case, joint center location errors were used to estimate the errors in the link lengths (Table 3), which were derived as the square root of the sum of squares of the inaccuracies in adjacent joint center locations.

2.4.4. Force plate measurements

Errors in force plate measurements manifest themselves in the actual measured ground reaction forces, as well as in the calculation of the center of pressure (COP) location and its relation to the ankle joint center. Force sensitivities were reported to be less than 1 N for the AMTI force plate and ±0.5% of the measured signal for a Kistler force plate. The magnitudes of the inaccuracies in the ground reaction measurements in present study were simply taken from force plate manuals (AMTI, model BP600900, Watertown, MA; Kistler, model 9281C, Winterthur, Switzerland). The COP location is derived from force plate measurements. In the "bottom-up" approach to inverse dynamics solutions for lower extremity joint torques, the measurement of distance between the COP and the center of rotation of the ankle joint can be subject to error. McCaw and Devita [11] analyzed this effect within the sagittal plane. They used inaccuracies of 5 and 10 mm in their sensitivity analysis. Schmiedmayer and Kastner [12] confirmed that the errors were less than 10 mm for most cases. We therefore used the values from McCaw and Devita (Table 3).

2.4.5. Motion marker noise and segmental accelerations

Inaccuracies in marker measurements due to noise in motion capture systems can influence the calculation of segment angle, segment acceleration (linear and angular), and the location of the joint center. Richards [6] performed a comparison of commercially available motion capture systems. Several system attributes were evaluated: for example, the ability to distinguish the distance between two rotating markers, measured as root-mean-square-error (RMSE), was 0.59 mm for the best performance system and 4.27 mm for the worst; the ability to determine the angle between three markers on a plate rotating at 60 rpm ranged from 1.42° to 4.43° as RMSE.

Studies quantifying the errors in acceleration values have been lacking and we were not able to identify any that reported error values per se. Inaccuracy data for angular acceleration were obtained from Cahouët et al. [29] who used the joint angular accelerations treated by a static optimization procedure as the benchmark and computed the relative RMSE in acceleration values calculated from marker measurements. These errors were reported to be 12.2% of the optimized acceleration at the ankle, 13% at the hip, and 6.2% at the shoulder joints.

Neither were we able to find any studies that assessed inaccuracies in linear acceleration. Therefore, we conducted an experiment to estimate the effect of motion capture system noise on the linear acceleration. The accelerations during free-falling marker trials were calculated and the mean value was found to be 9.74 ± 0.22 m/s^2. Since in general the acceleration of the center-of-mass is determined from motions of multiple markers, we used a formula from [30] to estimate the effect of a single marker error on the center-of-mass error. Further, the contribution of skin motion artifacts to this error was estimated by examining the difference in linear acceleration (instantaneous versus average) for a given segment. Average acceleration is an estimate of acceleration averaged over an initial time (t_o) to some final time (t_f), and is defined as the change in displacement (d) divided by the square of the change in time it took for the displacement to occur, i.e., $a_{ave} = (d_f - d_o)/(t_f - t_o)^2$. Using the maximum displacements of markers relative to the underline bone that were noted in past studies [13–15,25], we elected to calculate this difference in accelerations at two discrete time points. The time to reach peak displacement was observed to vary between one-third of the cycle and a full gait cycle [31–33], which corresponded to .37 and 1.1 s for an average gait cycle of 1.1 s as recorded in our experiment. A comparison of these differences in acceleration for each segment gave a relative error due to skin motion artifact in the measurement for each segment. Integration of the errors due to motion capture inaccuracies with errors due to skin motion artifacts led us to conclude that the total error in the acceleration ranges from 5% to 10%. Note that motion capture error magnitude may vary depending on the accuracy and repeatability of the equipment.

2.5. Synthesis of the inaccuracy magnitudes (Δx_i)

Because the reported values for Δx_i varied considerably across previous studies, two sets of Δx_i were formed to represent the range of values. The Δx_i values in these two sets are summarized in Tables 2 and 3. To synthesize these two sets, we address two particular issues that have plagued previous studies. First, inaccuracies have been reported in an inconsistent fashion: some studies have used the maximum error; others have reported RMSE values; still others have employed the standard deviation. We proposed the following convention in an attempt to unify the representations: the maximum error was assumed to be 3σ; the mean error was assumed to be zero so that the RMSE could be considered equivalent to one standard deviation (σ). Second,

Table 2
Two sets of inaccuracies (Set 1: small Δx_i, Set 2: large Δx_i) as percentages of respective nominal values for body segment parameters including the mass, center-of-mass location, and moment of inertia

	Mass		Moment of inertia		Center-of-mass	
	Set 1	Set 2	Set 1	Set 2	Set 1	Set 2
Thigh	5	12	5	14	5	11
Shank	5	5	5	26	5	6
Foot	5	36	5	47	5	15
Upper arm	5	13	5	16	5	16
Forearm + hand	5	10	5	20	5	5
Torso + head	5	12	5	37	5	14

Please cite this article in press as: Riemer R, et al., Uncertainties in inverse dynamics solutions: A comprehensive analysis and an application to gait, Gait Posture (2007), doi:10.1016/j.gaitpost.2007.07.012

Table 3
Inaccuracies associated with measurements

Segment length (mm)		Segment angle (degree)		Angular acceleration (%)		Segment COM linear acceleration (%)		Ground reaction force (%)		$Ankle_{COR}$-COP (mm)	
Set 1	Set 2	Set 1	Set 2	Set 1	Set 2	Set 1	Set 2	Set 1	Set 2	Set 1	Set 2
10	20	2, 4[a]	4, 8[b]	5	15	5	10	0.1	0.5	5	10

[a] Segment angle inaccuracy: shank, upper arm, forearm = 2°, torso and head, thigh = 4°.
[b] Segment angle inaccuracy: shank, upper arm, forearm = 4°, torso and head, thigh = 8°.

correlations between several of the input variables exist (e.g., joint center estimation impacts segments lengths and thus center-of-mass location, angles, angular acceleration and the COP to ankle joint center distance), although the exact forms of correlations are not known. To account for these correlations, we chose the error analysis formulation given in Eq. (4). This formulation computes the upper bound of the error while accommodating conditions where there may be correlations between input variable inaccuracies [18].

2.6. Gait experimental data acquisition

Gait data were collected on 10 subjects (five male and five female; body weight: 75.98 ± 14.74 kg; height: 1.69 ± 0.06 m; age 44 ± 8.7 years) to demonstrate the application of our analysis approach. For each subject, one walking trial at self-controlled normal speed with the right foot landing on the force plate (AMTI, model BP600900, Watertown, MA) was analyzed. The analyzed gait cycle was defined as heel strike to heel strike of the right foot starting with contact on the force plate. Motion data were obtained using a six-camera motion capture system with a sampling rate of 100 Hz (Vicon 460, Lake Forest, CA). The ground reaction force was sampled at rate of 100 Hz. Both marker motion and ground reaction data were low-pass filtered (Butterworth fourth-order forward and backward passes) with a cut-off frequency of 6 Hz for the motion and 15 Hz for ground reaction. The force and motion measurements were synchronized.

2.7. Data analysis

With the upper body (top-down) model, the elbow, shoulder, and bottom of the torso joints were analyzed during a full gait cycle, and calculation to determine the torque at the bottom of the torso included both arms. Due to the limitation of having one force plate, only the right-side joints (ankle, knee, and hip) were analyzed for the lower body (bottom-up) model during a full gait cycle. The bottom of the torso joint was analyzed during right leg single-support phase only.

All calculated joint torque and uncertainty values (obtained using two sets of Δx_i) for all joints were normalized in time as percentages of one gait cycle; using spline interpolation (MATLAB, version 6.5, The MathWorks, Inc., Natick, MA), and then normalized by a subject's height and weight. The mean and standard deviation of the joint torques and uncertainty values were then calculated for all subjects at each 1% time point of the gait cycle. To evaluate our approach, we examined whether the 3σ upper limit of the residual between torque values, calculated using the top-down and bottom-up models, was comparable to the uncertainty of the discrepancy predicted by the proposed approach. This discrepancy was equivalent to the residual or accumulated error at the free end of a chain-like linkage model (see proof in Appendix A).

We also investigated the temporal behavior of the estimated uncertainties, how they related to the calculated joint torques, and how the inaccuracies in each of the input variables contributed to the uncertainty in the results. To quantify the effect of uncertainty, the percentage of uncertainty relative to the joint torque was calculated by dividing the maximum estimated uncertainty by the peak torque.

3. Results

The uncertainties of the calculated joint torques were found to vary over time (Fig. 2). For the lower extremity joints especially the knee and hip, the uncertainties resemble the vertical ground reaction force profiles during the stance

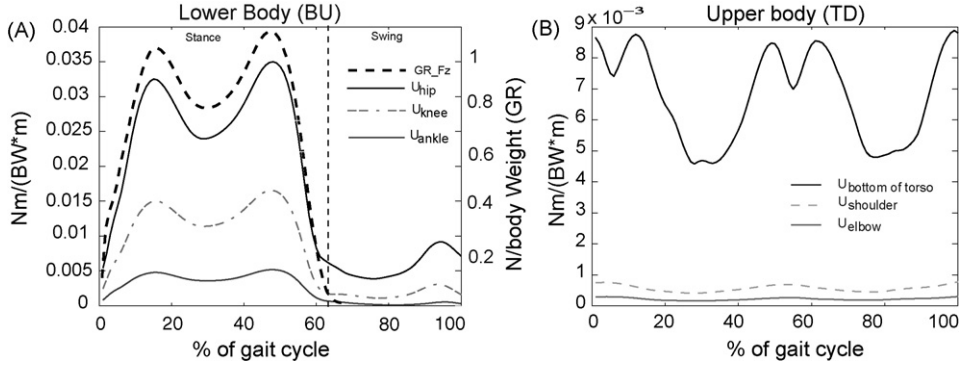

Fig. 2. Uncertainty estimates based on Set 1 inaccuracy values averaged across the 10 subjects: (A) uncertainties in leg joint torques in reference to the vertical ground reaction force GR_Fz (normalized by body weight); (B) uncertainties in upper body joint torques. Torques were normalized by body weight and height. Dashed vertical line indicates percentage at average toe-off.

Please cite this article in press as: Riemer R, et al., Uncertainties in inverse dynamics solutions: A comprehensive analysis and an application to gait, Gait Posture (2007), doi:10.1016/j.gaitpost.2007.07.012

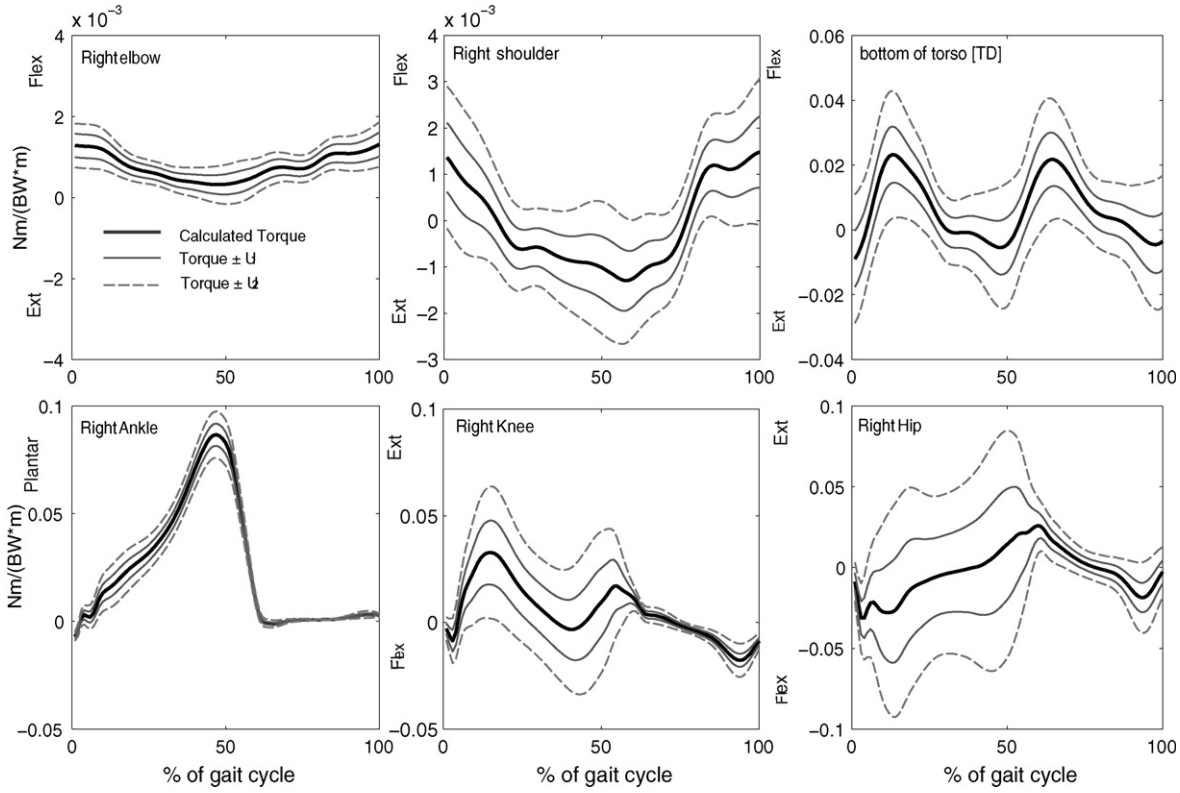

Fig. 3. Time-varying joint torque estimates (thick line) and $\pm U_1$, U_2 confidence limits (thin, and thin dotted lines, respectively) derived using Set 1 and 2 of inaccuracy values.

phase of the gait cycle (Fig. 2A). However, they do not seem to resemble the torque profiles (Fig. 3). Similar trends were observed for both sets of Δx_i. A test of the proposed approach (detail provided in Appendix) indicated that Set 1 inaccuracy values resulted in a closer prediction of the uncertainty in the solution than Set 2. The uncertainty magnitudes were smaller for the more distal joints, reflecting the nature of the error accumulation in the direction of recursive inverse dynamics computation.

The maximum values during the gait phase for the estimated uncertainties in the joint torques obtained using both the small and large sets of inaccuracies are summarized in Table 4. The values of the maximum estimated uncertainties relative to peak joint torque for the ankle, knee and hip are 6%, 50%, 114%, respectively, for Set 1 (small magnitude), and 12%, 105%, 232% for Set 2 (large magnitude). For the upper extremity joints, the bottom of the torso, shoulder and elbow are 38%, 50%, and 22% respectively, for Set 1, and 87%, 100% and 41% for Set 2.

Table 4
The maximum uncertainty values during a gait cycle, normalized by body weight (N) and height (m)

	Set 1 (small (x_i)		Set 2 (large (x_i)	
	Stance	Swing	Stance	Swing
Ankle	0.0052	0.0005	0.0108	0.0016
Knee	0.0165	0.0031	0.0342	0.0078
Hip	0.0352	0.0092	0.0720	0.0220
Bottom of torso (TD)	0.009		0.0205	
Shoulder	0.0008		0.0016	
Elbow	0.0003		0.00055	

Our analysis identified the main contributors that accounted for approximately 90% of the uncertainty in the joint torques (note that the contribution of the inaccuracy in an input to the output uncertainty can be considered as the product of function sensitivity and magnitude of the inaccuracy). In the upper body model, the main contributors were inaccuracies in segment angles (Fig. 4B). The inaccuracies in the segment angles are attributed mostly to the skin motion artifacts. For the lower body model, the main contributors were inaccuracies in the segment angles, the distance from the COP to the ankle center of rotation, and the foot mass (Fig. 4A). The secondary contributors for both top-down and bottom-up models include inaccuracies in the body segment parameters and accelerations.

4. Discussion

This paper describes a comprehensive analysis of the uncertainties (i.e., magnitude of possible errors) in joint torques from inverse dynamics solutions. The proposed approach was applied to the calculation of sagittal-plane joint torques during gait. Small and large estimates of inaccuracies in the input variables for the inverse dynamics

Please cite this article in press as: Riemer R, et al., Uncertainties in inverse dynamics solutions: A comprehensive analysis and an application to gait, Gait Posture (2007), doi:10.1016/j.gaitpost.2007.07.012

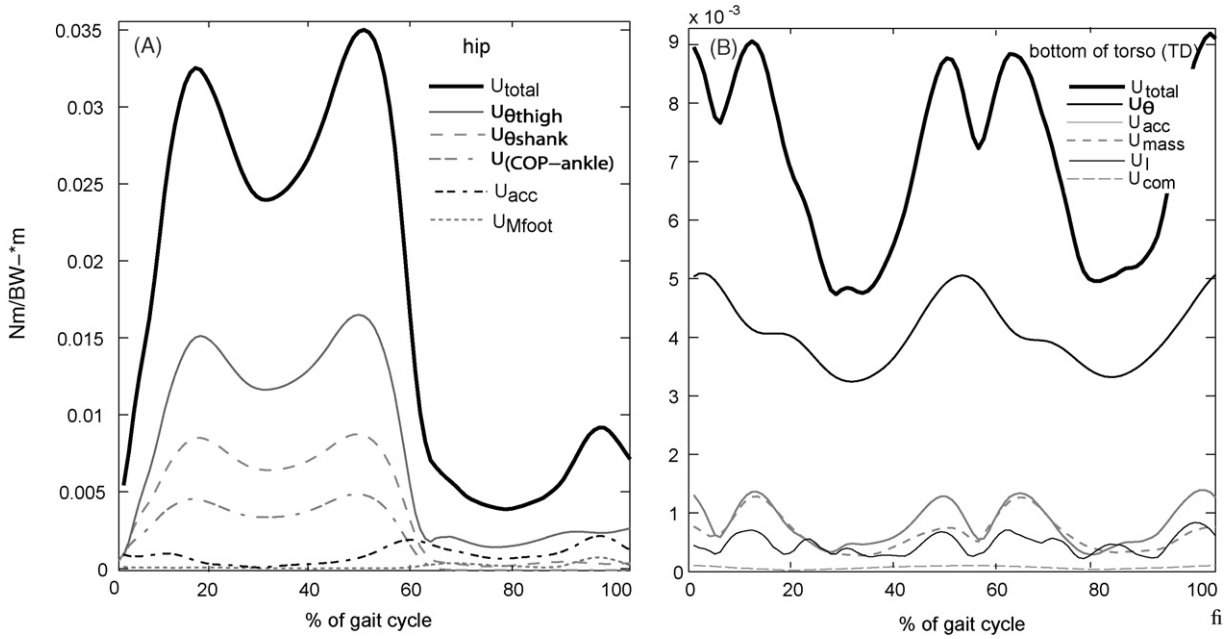

Fig. 4. Examples of main contributors to the estimated uncertainty (account for about 90%) in the joint torques (normalized by weight and height) using Set 1 inaccuracy values. (A) At the hip during the stance phase of the gait cycle (0–60%), inaccuracies in the (shank and thigh) segment angle measurements and the distance between the center of pressure and ankle center of rotation (COP-ankle) were the main contributors to uncertainty, and during the swing phase (60–100%) inaccuracy in the estimated foot mass became a significant contributing source. (B) At the bottom of the torso main contributors are inaccuracies in the torso angle measurements. Symbols for input variables: acc = acceleration; I = moment of inertia; COM = center-of-mass.

solutions were synthesized from the literature, and from our own set of complementary experimental data.

Following the conclusions of Andrews and Mish [34], we acknowledge that the results from our investigation are specific to the studied gait motion. It would be prudent not to assume that the same uncertainty magnitudes or main error contributors would apply to a lifting or jumping motion. However, the proposed analytical approaches are general and readily adaptable for movement-specific analyses.

The results of an experimental evaluation of the proposed approach (Appendix) validate its ability to predict realistic statistical bounds for the uncertainty in joint torque calculations, and suggest that for our experimental setup, the smaller inaccuracy values (Δx_i) in Set 1 correspond to more realistic estimation of the possible magnitude of error in the joint torque calculations. Since our experimental setting was rather generic, this conclusion may hold true for other gait studies employing inverse dynamics. The uncertainty estimations from the two inaccuracy sets showed similar trends. As can been seen in Table 4, the maximum uncertainty predicted by the large set (Set 2) is approximately twice as large as the uncertainty estimated using Set 1 across all joints.

An inspection of the estimated uncertainties in the torques relative to the peak torques suggests that the difference between the inverse dynamics solutions and the true values of joint torques at the knee, hip, elbow, shoulder, and the bottom of the torso can be substantial (from 6% to 232% of the maximum torque depending on the joint). The relatively large uncertainties in the torques should be considered when comparing the results from two different individuals or populations (e.g., symptomatic versus asymptomatic), and in experimental design to achieve, for example, desired statistical power.

Our analysis revealed that the uncertainties in joint torques were mainly influenced by the inaccuracies of a few key error sources. For the lower and upper extremity joints the main contributors to the total uncertainty were inaccuracies in segment angles. These inaccuracies are associated mainly with skin motion artifacts. This outcome agrees with the findings of [22,35], provides quantification of their conclusions, and shows how the uncertainty magnitudes for the major joints change over time during a gait cycle. As a side note, since using a common inaccuracy for segment length may not be appropriate for longer segments (e.g., thigh and torso), we reran our analysis such that the inaccuracies for these segments were increased by a factor of two. However, since inaccuracies in segment length have minimal contributions to the overall uncertainty, these modifications had nearly imperceptible changes to the overall uncertainty. Further work involving sensitivity analyses should examine how variations in individual error sources impact the overall uncertainty.

The substantial magnitudes of the possible errors or uncertainties in the joint torques, as unveiled in this study, underscore the importance of developing error correction methods for inverse dynamics solutions. Developments in the past decade have resulted in better measurement devices and filtering techniques that can and will continue to reduce

Please cite this article in press as: Riemer R, et al., Uncertainties in inverse dynamics solutions: A comprehensive analysis and an application to gait, Gait Posture (2007), doi:10.1016/j.gaitpost.2007.07.012

these errors. Errors in body segment parameters can be reduced by use of subject-specific geometric methods that integrate shape and density information [26,36] or image-based methods [25].

Furthermore, since the main contributors to error for lower extremity joints in the bottom-up solution were inaccuracies in the segment angles, it is particularly important to develop and apply a corrective method that compensates for skin movement artifacts. Two examples are the cluster method [37] and global optimization methods incorporating joint kinematic constraints [31–33]. Additional methods for general improvement of the solutions are those that exploit the "over-determined" nature of inverse dynamics computation when both kinematic and ground reaction force measurements are available [7,29,38]. The uncertainty information resulting from the current study can help refine some of the methods [7] and be used to derive a weighted, variability-dependent correction scheme.

It is acknowledged that not all possible sources of errors were investigated in our work. One source not included results from the rigid-body assumption. Rigid linkage models of the musculoskeletal system are idealized representations, while in fact the link lengths may vary significantly over time [39]. Additionally, rigid-body models may not be suitable for high impact movements [40]. Another possible error source intertwined with the issue of rigid-body representations is the lack of sufficient number of degrees of freedom in the model [41], which was not explicitly addressed in the current study.

Acknowledgements

This work was supported in part by an Office of Naval Research grant (N00014-03-0260). We also thank Daniel Bartlett, Matthew Major, Sang-Wook Lee for their constructive comments on earlier drafts of this manuscript.

Conflict of interest: None.

Appendix A. Error conservation in inverse dynamics

Here, we show that in inverse dynamics, the residual error at the end of a chain representation is equivalent to the difference between the bottom-up and top-down solutions at any given joint. The notational convention is illustrated Fig. A1.

The equation of motion for a given segment i can be expressed as:

$$I_i\boldsymbol{\theta}''_i = (\mathbf{d}_i \times \mathbf{f}_{j-1}) - (\mathbf{p}_i \times \mathbf{f}_j) + \boldsymbol{\tau}_{j-1} - \boldsymbol{\tau}_j. \quad \text{(A1)}$$

If we define the following term:

$$A_j = (\mathbf{d}_i \times \mathbf{f}_{j-1}) - (\mathbf{p}_i \times \mathbf{f}_j) - I_i\theta''_i, \quad \text{(A2)}$$

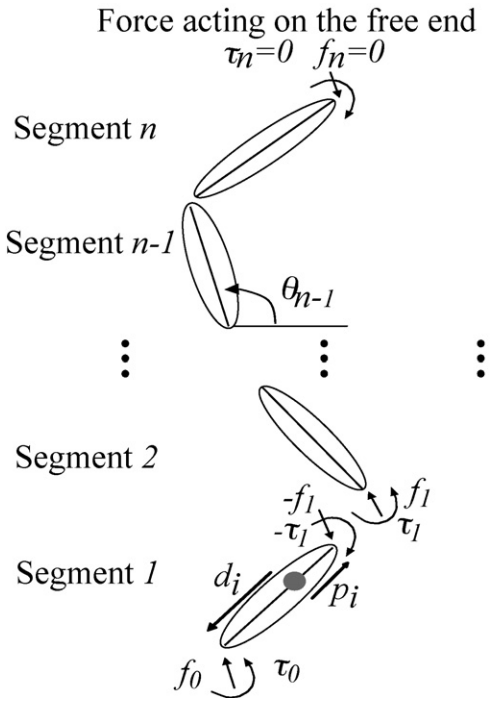

Fig. A1. A planar linkage model as the basis for recursive inverse dynamics, where $\boldsymbol{\tau}_j$ and $\boldsymbol{\tau}_{j-1}$ are the torques and $\mathbf{f}_j$ and $\mathbf{f}_{j-1}$ are force vectors at joint j and joint $j-1$ connected by segment i, θ_i is the angular position of segment i, $\mathbf{d}_i$ is the vector from the center-of-mass i to $\mathbf{f}_{j-1}$, and $\mathbf{p}_i$ is the vector from center-of-mass i to $\mathbf{f}_j$.

Eq. (A1) can then be simplified as:

$$\boldsymbol{\tau}_j = \tau_{j-1} + A_j \quad \text{(A3)}$$

Without the presence of error, the joint torques as inverse dynamics solutions in a bottom-up approach are computed as:

$$\text{Joint 1}: \quad \boldsymbol{\tau}_1 = \boldsymbol{\tau}_0 + A_1 \quad \text{(A4)}$$

$$\text{Joint 2}: \quad \boldsymbol{\tau}_2 = \boldsymbol{\tau}_1 + A_2 = \boldsymbol{\tau}_0 + A_1 + A_2 \quad \text{(A5)}$$

$$\vdots$$

$$\text{Joint } n: \quad \tau_n = \tau_0 + \sum_{j=1}^{n} A_j \quad \text{(A6)}$$

With the presence of errors (E_i), introduced at each step as $A_i \rightarrow A_i + E_i$, the joint torques become.

$$\text{Joint 1}: \quad \tilde{\tau}_1 = \tau_0 + (A_1 + E_1) \quad \text{(A7)}$$

$$\text{Joint 2}: \quad \tilde{\tau}_2 = \tilde{\tau}_1 + (A_2 + E_2)$$
$$= \tau_0 + (A_1 + E_1) + (A_2 + E_2) \quad \text{(A8)}$$

$$\vdots$$

$$\text{Joint } n: \quad \tilde{\tau}_n = \tau_0 + \sum_{j=1}^{n} A_j + \sum_{j=1}^{n} E_j \quad \text{(A9)}$$

Please cite this article in press as: Riemer R, et al., Uncertainties in inverse dynamics solutions: A comprehensive analysis and an application to gait, Gait Posture (2007), doi:10.1016/j.gaitpost.2007.07.012

The residual error at the end of the kinematic chain is

$$R = \tilde{\boldsymbol{\tau}}_n - \boldsymbol{\tau}_n. \tag{A10}$$

Substituting Eqs. (A6) and (A9) into Eq. (A10) results in

$$R = \left(\tau_0 + \sum_{j=1}^{n} A_j + \sum_{j=1}^{n} E_j\right) - \left(\tau_0 + \sum_{j=1}^{n} A_j\right), \tag{A11}$$

which reduces to

$$R = \sum_{j=1}^{n} E_j. \tag{A12}$$

For an arbitrary joint x, with the presence of error, the bottom-up solution takes the following general form:

$$\text{Joint } x: \quad \tilde{\tau}_x^{\mathrm{BU}} = \tau_0 + \sum_{j=1}^{x} A_j + \sum_{j=1}^{x} E_j \tag{A13}$$

In a top-down approach with the presence of error, the joint torque at joint $n-1$, which is the top-most joint, is computed as follows,

$$\text{Joint } n-1: \quad \tilde{\boldsymbol{\tau}}_{n-1}^{\mathrm{TD}} = \boldsymbol{\tau}_n - (A_n + E_n). \tag{A14}$$

For an arbitrary joint x, with the presence of error, the top-down solution takes the following form:

$$\text{Joint } x: \quad \tilde{\boldsymbol{\tau}}_x^{\mathrm{TD}} = \boldsymbol{\tau}_n - \left(\sum_{j=x+1}^{n} A_j + \sum_{j=x+1}^{n} E_j\right) \tag{A15}$$

The discrepancy (D) between the bottom-up and the top-down solutions at joint x, when errors exist, is:

$$D = \tilde{\boldsymbol{\tau}}_x^{\mathrm{BU}} - \tilde{\boldsymbol{\tau}}_x^{\mathrm{TD}} \tag{A16}$$

By substituting Eq. (A13) and (A15) into Eq. (A16), we get

$$D = \left(\tau_0 + \sum_{j=1}^{x} A_j + \sum_{j=1}^{x} E_j\right) - \left(\tau_n - \left(\sum_{j=x+1}^{n} A_j + \sum_{j=x+1}^{n} E_j\right)\right) \tag{A17}$$

which can be simplified to

$$D = \sum_{j=1}^{n} E_j. \tag{A18}$$

Thus, by comparing Eqs. (A12) and (A18), we conclude the residual R accumulated at the end of a linkage model is equal to the discrepancy between the bottom-up and the top-down torque solutions at any joint in the linkage. This equality also reflects that total error accumulation in inverse dynamics by going through the same number of recursive steps, regardless of the direction, is conserved in the system. We term this as error conservation in the inverse dynamics.

Appendix B. Evaluation of proposed approach by a comparison of the top-down and bottom-up results

While the true errors associated with inverse dynamics solutions are never known, it is possible to estimate the maximum errors in calculated joint forces and torques. The residual at the free-end of a kinematic chain is the accumulated error in an inverse dynamics computation. Note that the uncertainty is the upper bound of the possible error, so if the predicted uncertainty at the end of a kinematic chain is comparable in magnitude and bounds the residual, it would lend credence to the error analysis results.

As shown above in Appendix A, the discrepancy between the torque values calculated by the bottom-up and top-down approaches ($D = \tau_B - \tau_T$) at any joint is equivalent to the residual or accumulated error in the free-end of a chain. Choosing the joint at the bottom of the torso as a point for comparison, we calculated the uncertainty in the discrepancy between values from the two approaches (U_D) and compared it to the 3σ statistical upper bound of the calculated residual ($D_{3\sigma}$) defined as:

$$D_{3\sigma} = 3 \times \mathrm{SD}(\tau_B - \tau_T), \tag{B}$$

where $\mathrm{SD}(\tau_B - \tau_T)$ is the standard deviation of the difference in the torque values at the bottom of the torso obtained with the bottom-up and top-down approaches, respectively. The standard deviation was calculated by averaging, over all subjects, the discrepancies in torques for each subject at each (one percentage) point during the gait cycle.

Uncertainties were calculated for both sets of inaccuracies (U_{D1} and U_{D2} for Set 1 and Set 2, respectively). Therefore, if the proposed approach has merit, then $D_{3\sigma}$

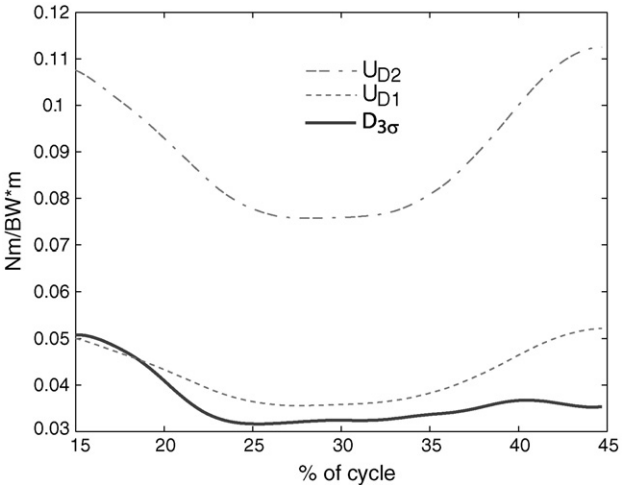

Fig. B1. The statistical upper limit for the discrepancy ($D_{3\sigma}$) between the torque values derived using the top-down and bottom-up models is bounded by the estimates of uncertainty in the discrepancy (U_{D1} and U_{D2} obtained using Set 1 and Set 2 of (x_i). Data are averages across all subjects and during the stance phase of the right leg.

Please cite this article in press as: Riemer R, et al., Uncertainties in inverse dynamics solutions: A comprehensive analysis and an application to gait, Gait Posture (2007), doi:10.1016/j.gaitpost.2007.07.012

should be of similar magnitude as and upper-bound by U_{D1} or U_{D2}. This discrepancy analysis was performed only during the single-support phase of the right leg, due to the limitation of having only one force plate.

The discrepancy between the torque values ($D_{3\sigma}$) was found to be upper-bounded by the uncertainties in the discrepancy associated with both the small and large set of inaccuracies (Fig. B1). This suggests that an upper bound on the error in the joint torque values may be realistically predicted by our approach. Further, it appears that for our experimental setup, the set of the smaller inaccuracy values (U_{D1}) resulted in a closer prediction of the uncertainty in the solution.

References

[1] Winter DA. Biomechanics and motor control of human movement. Hoboken, New Jersey: John Wiley and Sons; 2005.
[2] Challis JH. Accuracy of human limb moment of inertia estimations and their Influence on resultant Joint moments. J Appl Biomech 1996;12:517–30.
[3] Kingma I, Toussaint HM, De Looze MP, Van Dieen JH. Segment inertial parameter evaluation in two anthropometric models by application of a dynamic linked segment model. J Biomech 1996;29(5):693–704.
[4] Pearsall DJ, Costigan PA. The effect of segment parameter error on gait analysis results. Gait Posture 1999;9(3):173–83.
[5] Ganley KJ, Powers CM. Determination of lower extremity anthropometric parameters using dual energy X-ray absorptiometry: the influence on net joint moments during gait. Clin Biomech 2004;19(1):50–6.
[6] Richards JG. The measurement of human motion: a comparison of commercially available systems. Hum Movement Sci 1999;18(5):589–602.
[7] Kuo AD. A least-squares estimation approach to improving the precision of inverse dynamics computations. J Biomech Eng 1998;120(1):148–59.
[8] Bell AL, Pedersen DR, Brand RA. A comparison of the accuracy of several hip center location prediction methods. J Biomech 1990;23(6):617–21.
[9] Leardini A, Cappozzo A, Catani F, Toksvig-Larsen S, Petitto A, Sforza V, et al. Validation of a functional method for the estimation of hip joint centre location. J Biomech 1999;32(1):99–103.
[10] Schwartz MH, Rozumalski A. A new method for estimating joint parameters from motion data. J Biomech 2005;38(1):107–16.
[11] McCaw ST, DeVita P. Errors in alignment of center of pressure and foot coordinates affect predicted lower extremity torques. J Biomech 1995;28(8):985–8.
[12] Schmiedmayer H-B, Kastner J. Enhancements in the accuracy of the center of pressure (COP) determined with piezoelectric force plates are dependent on the load distribution. J Biomech Eng 2000;122(5):523–7.
[13] Cappozzo A, Catani F, Leardini A, Benedetti MG, Della Croce U. Position and orientation in space of bones during movement: experimental artefacts. Clin Biomech 1996;11(2):90–100.
[14] Holden JP, Orsini JA, Siegel KL, Kepple TM, Gerber LH, Stanhope SJ. Surface movement errors in shank kinematics and knee kinetics during gait. Gait Posture 1997;5(3):217–27.
[15] Stagni R, Fantozzi S, Cappello A, Leardini A. Quantification of soft tissue artefact in motion analysis by combining 3D fluoroscopy and stereophotogrammetry: a study on two subjects. Clin Biomech 2005;20(3):320–9.
[16] Desjardins P, Plamondon A, Gagnon M. Sensitivity analysis of segment models to estimate the net reaction moments at the L5/S1 joint in lifting. Med Eng Phys 1998;20(2):153–8.
[17] De Leva P. Adjstments to zatsiorsky-seluyanov's segment inertia parameters. J Biomech 1996;29(9):1223–30.
[18] Taylor JR. An introduction to error analysis: the study of uncertainties in physical measurements. Sausalito, California: University Science Books; 1997.
[19] Cerveri P, Pedotti A, Ferrigno G. Kinematical models to reduce the effect of skin artifacts on marker-based human motion estimation. J Biomech 2005;38(11):2228–36.
[20] Cappozzo A, Della Croce U, Leardini A, Chiari L. Human movement analysis using stereophotogrammetry. Part 1. Theoretical background. Gait Posture 2005;21(2):186–96.
[21] Chiari L, Della Croce U, Leardini A, Cappozzo A. Human movement analysis using stereophotogrammetry. Part 2. Instrumental errors. Gait Posture 2005;21(2):197–211.
[22] Leardini A, Chiari L, Della Croce U, Cappozzo A. Human movement analysis using stereophotogrammetry. Part 2. Soft tissue artifact assessment and compensation. Gait Posture 2005;21(2):212–25.
[23] Della Croce U, Leardini A, Chiari L, Cappozzo A. Human movement analysis using stereophotogrammetry. Part 4. Assessment of anatomical landmark misplacement and its effects on joint kinematics. Gait Posture 2005;21(2):226–37.
[24] Cappozzo A, Berme N. Subject specific segment inertial parameter determination: a survey of current methods. In: Berme N, Cappozzo A, editors. Biomechanics of human movement applications in rehabilitation, sports and ergonomics. Worthington, Ohio: Bertec Corporation; 1990. p. 179–85.
[25] Durkin JL, James JDB, Andrews DM. The measurement of body segment inertial parameters using dual energy X-ray absorptiometry. J Biomech 2002;35(12):1575–80.
[26] Hatze H. A mathematical model for the computational determination of parameter values of anthropomorphic segments. J Biomech 1980;13(10):833–43.
[27] Roux E, Bouilland S, Godillon-Maquinghen AP, Bouttens D. Evaluation of the global optimisation method within the upper limb kinematics analysis. J Biomech 2002;35(9):1279–83.
[28] Davis III RB, Ounpuu S, Tyburski D, Gage JR. A gait analysis data collection and reduction technique. Hum Movement Sci 1991;10(5):575–87.
[29] Cahouet V, Luc M, David A. Static optimal estimation of joint accelerations for inverse dynamics problem solution. J Biomech 2002;35(11):1507–13.
[30] Cappozzo A, Cappello A, Della Croce U, Pensalfini F. Surface-marker cluster design criteria for 3-D bone movement reconstruction. IEEE Trans Biomed Eng 1997;44(12):1165–74.
[31] Cheze L, Fregly BJ, Dimnet J. A solidification procedure to facilitate kinematic analyses based on video system data. J Biomech 1995;28(7):879–84.
[32] Lu TW, O'Connor JJ. Bone position estimation from skin marker coordinates using global optimisation with joint constraints. J Biomech 1999;32(2):129–34.
[33] Reinbolt JA, Schutte JF, Fregly BJ, Koh BI, Haftka RT, George AD, et al. Determination of patient-specific multi-joint kinematic models through two-level optimization. J Biomech 2005;38(3):621–6.
[34] Andrews JG, Mish SP. Methods for investigating the sensitivity of joint resultants to body segment parameter variations. J Biomech 1996;29(5):651–4.
[35] Cappozzo A. Three-dimensional analysis of human walking: experimental methods and associated artifacts. Hum Movement Sci 1991;10(5):589–602.
[36] Yeadon MR. The simulation of aerial movement II. A mathematical inertia model of the human body. J Biomech 1990;23(1):67–74.
[37] Alexander EJ, Andriacchi TP. Correcting for deformation in skin-based marker systems. J Biomech 2001;34(3):355–61.

Please cite this article in press as: Riemer R, et al., Uncertainties in inverse dynamics solutions: A comprehensive analysis and an application to gait, Gait Posture (2007), doi:10.1016/j.gaitpost.2007.07.012

[38] Vaughan CL, Andrews JG, Hay JG. Selection of body segment parameters by optimization methods. J Biomech Eng 1982;104(1): 38–44.
[39] Zhang X, Lee S-W, Braido P. Towards an integrated high-fidelity linkage representation of the human skeletal system based on surface measurement. Int J Ind Ergo 2004;33(3):215–27.
[40] Gruber K, Denoth J, Stuessi E, Ruder H. The wobbling mass model. In: Jonsson B, editor. Biomechanics X-B. Champaign, IL: Human Kinetics; 1987. p. 1095–9.
[41] Cappozzo A. Minimum measured-input models for the assessment of motor ability. J Biomech 2002;35(4):437–46.

Please cite this article in press as: Riemer R, et al., Uncertainties in inverse dynamics solutions: A comprehensive analysis and an application to gait, Gait Posture (2007), doi:10.1016/j.gaitpost.2007.07.012